Desalination and Water Treatment
www.deswater.com

doi: 10.5004/dwt.2020.25761

192 (2020) 248–258
July

Delineation of groundwater potential zones using integrated remote sensing, GIS and multi-criteria decision making (MCDM)

Basheer A. Elubid[a,b,*], Tao Huang[a], Dao-Ping Peng[a], Ekhlas H. Ahmed[c], Mohammed M. Babiker[d]

[a]*Department of Environmental Science and Engineering, Faculty of Geosciences and Environmental Engineering, Southwest Jiaotong University, high-tech zone, Chengdu 611756, China, Tel. +8615208214309/+8617308094289; emails: basheer@my.swjtu.edu.cn/ elubaid@yahoo.com (B.A. Elubid), taohuang70@126.com (T. Huang), pdp0330@qq.com (D.-P. Peng)*
[b]*Department of Hydrogeology, Faculty of Petroleum and Minerals, Al Neelain University, Khartoum 11121, Sudan*
[c]*School of Resources and Environment, University of Electronic Science and Technology of China, Chengdu 611756, China, email: ekhlasgeo81@yahoo.com (E.H. Ahmed)*
[d]*Water Environmental Sanitation Project (WES), Gedaref State Water Corporation, Gedaref–32214, Sudan, email: ahmed_geonuv@163.com (M.M. Babiker)*

Received 25 August 2019; Accepted 27 February 2020

ABSTRACT

This study aimed to delineate the groundwater potential zones (GWPZ) through the integrations of remote sensing (RS), geographical information system (GIS), and multi-criteria decision making (MCDM). In this case, the RS and GIS were used to produce the hydrogeological thematic layers, that is, geomorphology, slope, geology, land use, lineaments, and drainage. Therefore, the weighting of each thematic layer was done by the weighted overlay technique in the ArcGIS environment and normalized by the MCDM technique. The results consequently acquired from the integration of the various thematic maps were then cross-checked with an electrical resistivity of the subsurface layers and boreholes data; it was produced a good match with the GWPZ model. The final map of the area was demarcated by four different GWPZ, namely, very good (11.03%), good (38.44%) poor (37.33%), and very poor (13.20%) of the Shemeliab watershed area. The outcomes of this research are advantageous to the decision-makers of the water management for locating suitable positions of new production wells for their target areas. The process and findings of this study also could be used for improving plans for potential utilization of the groundwater resources in other regions of the same geological, hydrogeological, and environmental conditions.

Keywords: Boreholes data; Electrical resistivity; Subsurface lithology; Thematic layers

1. Introduction

Groundwater investigation is growing more and became essential nowadays to meet the multiple needs of water supply for drinking, industrial and agriculture sectors, especially in areas where surface water supply is not sufficient for human consumption and agricultural uses. [1,2]. Water scarcity is a well-known problem, especially in basaltic rock terrain and high-dense clay soil, where rainfall has runoff considerably without percolating to groundwater.

Through the most recent couple of decades, a great interest in utilizing remote sensing (RS) and geographical information system (GIS) techniques for groundwater potential zones (GWPZ) has been made by numerous specialists all over the world [3–6]. The GWPZ can be delineated through different hydrogeological thematic layers that are,

* Corresponding author.

[7] depend only on lineaments for groundwater exploration, [8] used the applications of RS, GIS, and analytic hierarchy process techniques (AHP), when others integrated various thematic layers, that is, geomorphology, slope, drainage, land use/land change, and soil texture [9,10]. The use of RS data and GIS techniques compound with field check and observations are well known as a useful method for groundwater mapping and exploration [11].

Delineation of potential groundwater zones with geophysical methods has gained extensive interest in the last few decades [12]. Electrical resistivity tomography (ERT) is one of the geophysical methods most essential used in exploring the subsurface lithology [13]. The electrical resistivity technique has broad usage in environmental, engineering, and shallow aquifers investigation [14].

Over the last 10 y, urbanization in Sudan has increased the urban population three times higher increase in the past [15], this leads to aggravated long suffered from an acute scarceness of water especially in the study area. Our study area lies eastern Gedaref town east-central Sudan, between latitudes 13° 9′ 00″ N and 14° 22′ 00″ N and longitudes 35° 11′ 00″ E and 36° 13′ 00″ E. Shemeliab watershed area is one of the agricultural centers of seeds producing in Sudan [16], it consists six localities of population settlement, Sharafa, El Ogol, Weheshat, Umm shagara, Ruffah, and Shemeliab. Geomorphologically, the Shemeliab watershed area characterized by flat plain with some elevated areas. The area suffers from an intense lack of water, particularly in the summer period.

Different type of researches were accomplished around Shemeliab area, for example; the basaltic rocks of Gedaref were classified as one of volcanism assemblage in the north-eastern part of Sudan as Alkaline basalt by [17], the geology of Gedaref have been revealed by [18] during his study of the Afro Arabian dome, [19] interpreted the data of gravity to estimate the groundwater occurrences in the eastern part of Sudan, which indicated the presence of a rifted structure trending northwest with a considerable thickness near the study area, the groundwater quality of Gedaref area was studied by [20]; they have classified it into two major groups as; $NaHCO_3$ for the sandstone aquifers and alkaline group for the basaltic aquifers, while [21] studied the West part of Gedaref city and created a conceptual model for the hydrogeologic system in the area, [22] assessed the first palynological outcome from the study of terrestrial fossils of subsurface layers in Gedaref formation, Also the new finding of trace fossils has been studied by [23] in which they described for the first time, bioturbated layers in some sedimentary outcrops of Gedaref town, according to [24]; nine sedimentary facies were identified near Shemeliab.

The main goal of this study was to map and define potential groundwater zones in the Shemeliab watershed area by applying RS and GIS coupled with other hydrogeological parameters. Our study established on the integration of RS, GIS and multiple-criteria analysis techniques to determine the GWPZ; through the multi-thematic layers such as geomorphology, slope, geology, land use/land cover, lineament density, and drainage density. The novelty in this work is determining the potential groundwater zone from the weighted overlay to generate the GWPZ model in the study area. However, the developed model validation was checked against the interpreted geophysical data and the boreholes data, in this case, the interpolation of the geophysical interpretation was reproduced as a polygon feature class using ArcGIS software. Moreover, the geophysical resistivity method was used to dedicate the thin basaltic layers intruded with sandstone layers.

Access to groundwater is charming increasingly difficult in areas of high-dens clay cover and fast urbanization. For this, the presented approach is not only applicable to the Shemeliab watershed area, but also to many other regions that have the same environmental and geological situations. Although there were some other studies applied around the study area, no other study was conducted to define potential groundwater zones using this technique in or around the Shemeliab area.

2. Methods

2.1. Study area and regional geological setting

The regional geology of the Shemeliab area and its surroundings are shown in Fig. 1 consists mainly of basement complex terrain [23,25]. The basement composed various igneous and metamorphosed lithological units dominantly in the south and basaltic volcanic flows which mostly covered by younger sediments. The major rock units cropped out as isolated hilly or low-lying outcrops within the intervening clay-covered. Thick clayey overburden covers most of the Shemeliab area which is characterized by flat plain with some elevated areas. The high regions around Shemeliab consist of Oligocene basalt and other two sedimentary sections [23], one is located near Shemeliab some far 15 km at Umm Khanjar villages, and the other at Al Hamra of far distance about 60 km from the study area.

2.2. Data sources and thematic maps production

This study is established on the integration of several thematic layers into RS and GIS platforms for an outfit the spatial database. The methodology flowchart of this study is given in Fig. 2.

2.2.1. Toposheets and base maps

Topographic sheets and geological map of Geological Research Authority of Sudan has been modified for regional geological mapping of the study area. However, these maps can't distinguish the other geological units of the small scale, thus, the field survey check has been used to identify the unmappable geological units to generate the detailed geological map.

2.2.2. RS data

Landsat-7 ETM+ data (Path 171-Row 050), dated 03 October 2017 were used through different steps of image processing and enhancement. The satellite image was performed to produce the false-color composite (FCC) through a combination of the three bands that is, 4, 3, and 2 as red, green, and nlue (RGB), which was applied to provided land use/land cover map. The generated FCC was applied also to supplement the geomorphological map of

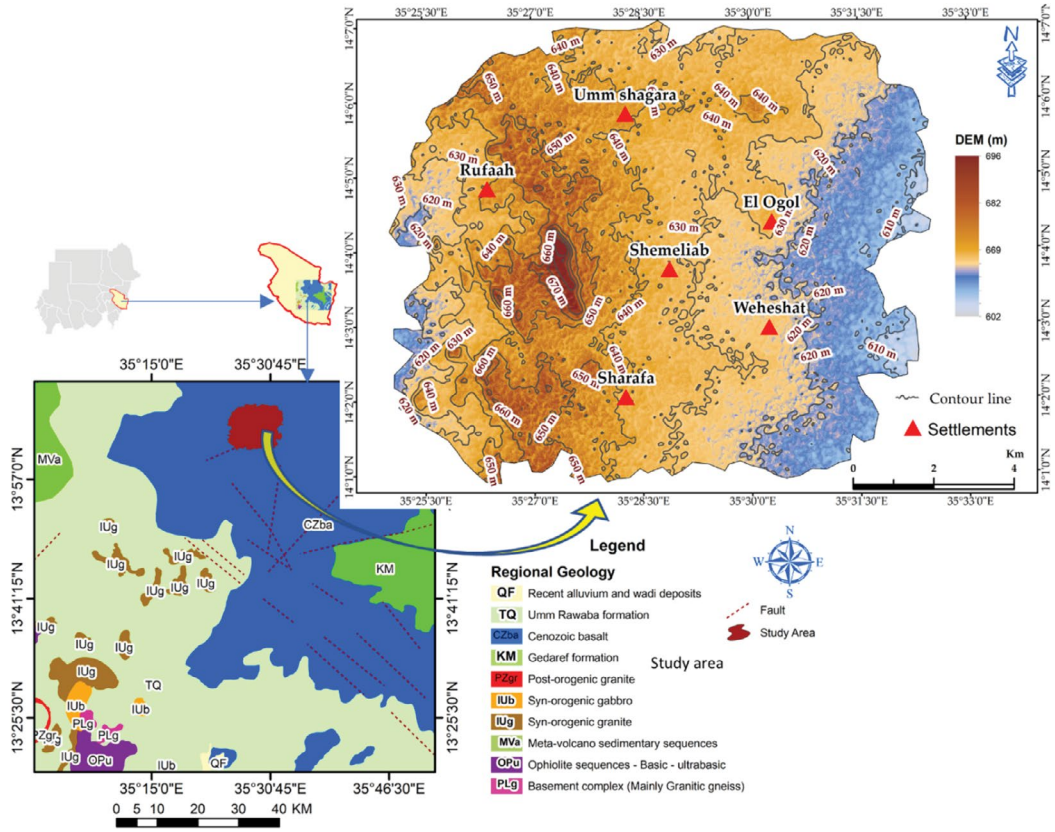

Fig. 1. Location and regional geology of the Shemeliab watershed area.

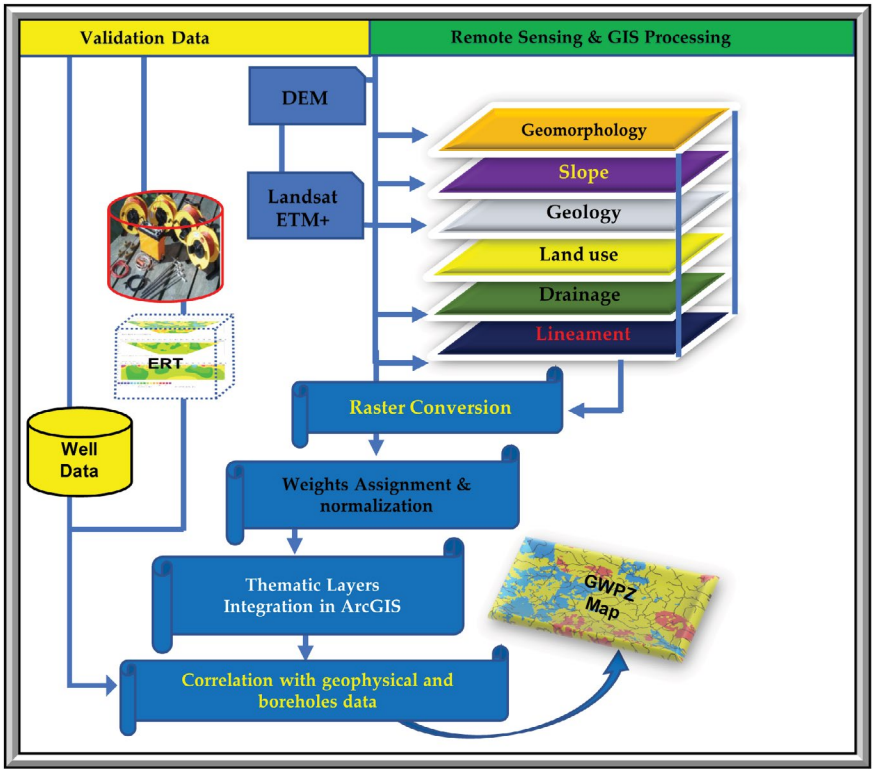

Fig. 2. Methodology flowchart.

the area. digital elevation model (DEM) of the Shemeliab watershed was extracted from Shuttle Radar Topographic Mission (SRTM) data downloaded from the US Geological Survey website (https://earthexplorer.usgs.gov/). The SRTM DEM data was processed, then has been used to provide topographic and slope maps of the area. From the DEM data coupled with satellite image, the drainage lines were calculated and digitized then, the lineaments were used to prepare drainage density maps of the watershed area. The generate watershed order of Global Mapper was used to implement a watershed boundary to detect the stream paths as well as delineate the sub-watershed areas that drain into a specific stream passage. Finally, the drainage density (D_d) was calculated as:

$$D_d = \frac{\sum_{i=1}^{n}(\mathrm{SL}_i)}{A} \tag{1}$$

where D_d is the drainage density (km km^{-2}), SL is the cumulative length (km) of all streams present within 'A' area, A is the area (km^2), and n is the total number of streams present within the area 'A'.

2.2.3. Geophysical resistivity information and boreholes data

The resistivity survey of the investigation conducted through two denomination field methods. These methods are vertical electrical sounding (VES) for vertical variations and horizontal electrical profiles (HEP), for lateral variations. Eleven VES was conducted in the Shemeliab watershed area to investigate the groundwater aquifer's characteristics and to realize the variation of subsurface lithology. The ERT was used to form the geometry of the subsurface geology (lithology units and groundwater zones). The resistivity profiles handled in the Shemeliab area were oriented to cross the target fractures (release and extensional fractures).

The information related to the boreholes of the study area, that is, lithological units, depths to bedrock were collected from the field during the geophysical survey, where the yield data of available wells were collected from the water corporation of Gedaref State – Sudan and water environmental sanitation, Project Gedaref State – Sudan.

2.3. Assigned and normalized weights of different features

The concept of assignment and normalization of weights for this study has been obtained through a different selection of international expert studies in hydrological issues over the world. The approach developed by using Saaty's AHP techniques [26] to complete the weights assigned to various themes and their features used in GWPZ. The calculation of the consistency rate includes the following steps:

- *Step 1*: Calculation of principal eigenvalue (λ) using the eigenvector method.

$$\mathrm{CI} = \frac{\lambda_{\max} - n}{n-1} \tag{2}$$

where n is the number of criteria or factors, CI is consistency Index.

- *Step 2*: computation of the consistency ratio (CR)

$$\mathrm{CR} = = \frac{\mathrm{CI}}{\mathrm{RCI}} \tag{3}$$

where RCI refers to a random consistency index.

In the current study, six themes were evaluated: (i) geomorphology, (ii) slope, (iii) geology, (iv) land use, (v) lineaments, and (vi) drainage. Thus, the vector layers, were transformed to raster layers for integrating with other raster thematic layers for GIS modeling process. A resampling process has been generated for all the thematic layers to match the same resolution. Each theme has a weight value according to its power of impact/contributing across the groundwater reserve. Then, each feature of an individual theme, in turn, has been figured in a 1–10 scale in ascending order of hydrogeological indications. A value of 10 is assigned to features of highest effects, and 1 for the lowest one.

The performance of groundwater potential index (GWPI), taking all the features into account, was calculated as:

$$\mathrm{GWPI} = \mathrm{Gm}_w\mathrm{Gm}_r + \mathrm{Sl}_w\mathrm{Sl}_r + \mathrm{Geo}_w\mathrm{Geo}_r + \mathrm{Lu}_w\mathrm{Lu}_r + \mathrm{DD}_w\mathrm{DD}_r + \mathrm{LD}_w\mathrm{LD}_r \tag{4}$$

where Gm = Geomorphology, Sl = Slope, Geo = Geology, Lu = Land use/land cover, DD = Drainage density, LD = Lineaments density, X_{wr} the (w) = weight of the theme and (r) = rank of the theme.

2.4. GWPZ verification

The map of GWPZ delineated in this study was verified using the applied geophysical data and the available well data. Thus, the results obtained from the integration of different thematic maps were correlated with geophysical and boreholes data, in which boreholes and geophysical data were overlaid on the final groundwater probability zone map to examine the accuracy of the current work in the various groundwater prospective zones.

3. Results and discussion

3.1. Thematic layers of Shemeliab watershed

The groundwater occurrence in the Shemeliab area is controlled by geological and hydrogeological factors, which were represented as six layers of geomorphology, slope, geology, land use, lineaments, and drainage.

3.1.1. Geomorphology

Geomorphologically, the Shemeliab watershed characterized by flat plain with some elevated areas; distinguished by attracting attention water divide bearings North-South direction. The general altitude is about 570 to more than 700 m above mean sea level (a.m.s.l). The geomorphology is one of the most important features in estimating the

groundwater potential zones. The hydrogeomorphology in the Shemeliab area is highly affected by the structures and lithological units of the area. Material related to river/water-bodies and buoyant floodplain has higher water content capability and subsequently assigned the best landform for high groundwater potential.

The geomorphology of the Shemeliab area (Fig. 3a), in which the excellent groundwater prospect reflected on the flood plain are on the Eastern part and water-bodies in the Western part. The alluvial plain zone covers a plurality of the Shemeliab area, and the groundwater content in these zones is limited due to less recharge caused by clay cover.

3.1.2. Slope

The slope has its importance and essential role in affecting the control of the run-off, recharge, and movement of the surface water. The groundwater recharge depends on many factors, the slope is one of these factors. Regions of flat land could be categorized as 'very good' with comparatively high infiltration rate, while the regions with moderate slope are deemed as 'good' for groundwater recharge because of a little fluctuate topography. The relatively high run-off and low percolated surface-water are observed in the areas of the steeper slope, and hence are assorted as 'poor' and have less groundwater storage. DEM of the Shemeliab watershed was extracted from SRTM to generate the slope map of the study area, Fig. 3b. The lower percent slope was allocated higher grade or rank because it allows more groundwater retention and less run-off, while the higher one was assigned lesser rank due to more run-off and less infiltration.

3.1.3. Detailed geology

The detailed geology of the Shemeliab watershed area depicted in Fig. 3c, consists of four geological units that can be mentioned in ascending order as (i) Gedaref formation (sandstone), (ii) Gedaref formation (mudstone), (iii) Cenozoic basalt, and (iv) recent alluvium and wadi deposits. Gedaref formation involving (sandstone - mudstone) and recent alluvium and wadi deposits have been given higher weight as compared to Cenozoic basalt.

3.1.4. Land use/land cover

The land use/land cover categories were mapped out from Landsat Enhanced Thematic Mapper Plus (ETM+) of Landsat 7 with acquisition date 2006/12/17, covering Path-171 and Row-050 were used for image classifications. However, in this case, we used band 4, 3 & 2 as RGB for image color composite. The satellite image of Landsat image has a certain limitation due to the low spatial resolution, which may not be able to acquire some of the image objects. However, Google Earth imagery and field investigations data were used to reduce this limitation to provide better interpretations in mapping land uses.

The land-use types in the study area (Fig. 3d) are cropland, settlement, bare soil, open forest, and water bodies. The land wrapped by forest regulates continuous water flow, and water percolation regularly, while the cultivated land influence the slope stability owing to the saturation of covered soil.

3.1.5. Drainage density

The drainage lines are shown in Fig. 3e; have been generated from the digital elevation model (DEM) using several algorithms and were applied for acquisition of the drainage density map. The area characterized by dendritic drainage pattern, which indicates the resistance of the substrata or rocks was uniform to weathering and erosion. High drainage density amounts were causing a high surface water runoff, and thus mark low groundwater potential zone, when the low drainage density gives high ranks according to their high potentiality to groundwater recharge.

3.1.6. Lineament density

Landsat ETM+7 image was digitally enhanced utilizing different handling techniques, particular confirmations were given to image filtering, by which linear features were revealed. Filtration can be classified into directional and non-directional filtering, the better one is the directional filter because it's the ability to enhances and highlight more lineaments in specific direction than the non-directional filtering, whereas nondirectional filter has efficiency with all lineaments features that oriented in several directions. The goal of the directional filtering process used here is to detect the lineaments and classified them according to their bearings. The outcomes of the lineament's interpretation are shown as lineaments density map in Fig. 3f.

The groundwater occurrence in the Shemeliab area is dominated by several factors and each factor is assigned a weight depending on its influence on surface water percolation, movement, and storage of groundwater. In the present study, the weighted values were given as 8, 7, 6, 5, 3 and 2 to geology, geomorphology, lineament density, land use/land cover, drainage density, and slope respectively (Table 1), depending on their effects and control on GWPZ.

The integration of thematic layers was brought out as a GWPZ map which helped to demarks the GWPZ effectively in the study area. From the analysis, the GWPZ with very good, good, poor, and very poor prospects covering the whole watershed area has been demarcated and are shown in Fig. 4. The output potential model detects that the very good and good (high potential zones) occur in Northwest, Southwest, and middle-east parts (sedimentary and wadi deposits area). The poor potential zones spread in all parts of the study area. The very poor potential zones occur in Southwest, Northeast, and central parts as moderate to small patches.

3.2. Validation of extracted GWPZ using geophysical resistivity information and boreholes yield

The validation and accuracy of the final extracted GWPZ were aims to layout a clear output related to the groundwater condition of the Shemeliab watershed area. For this investigation, the geophysical survey and the well inventory data represents the sustainable phase of data acquisition.

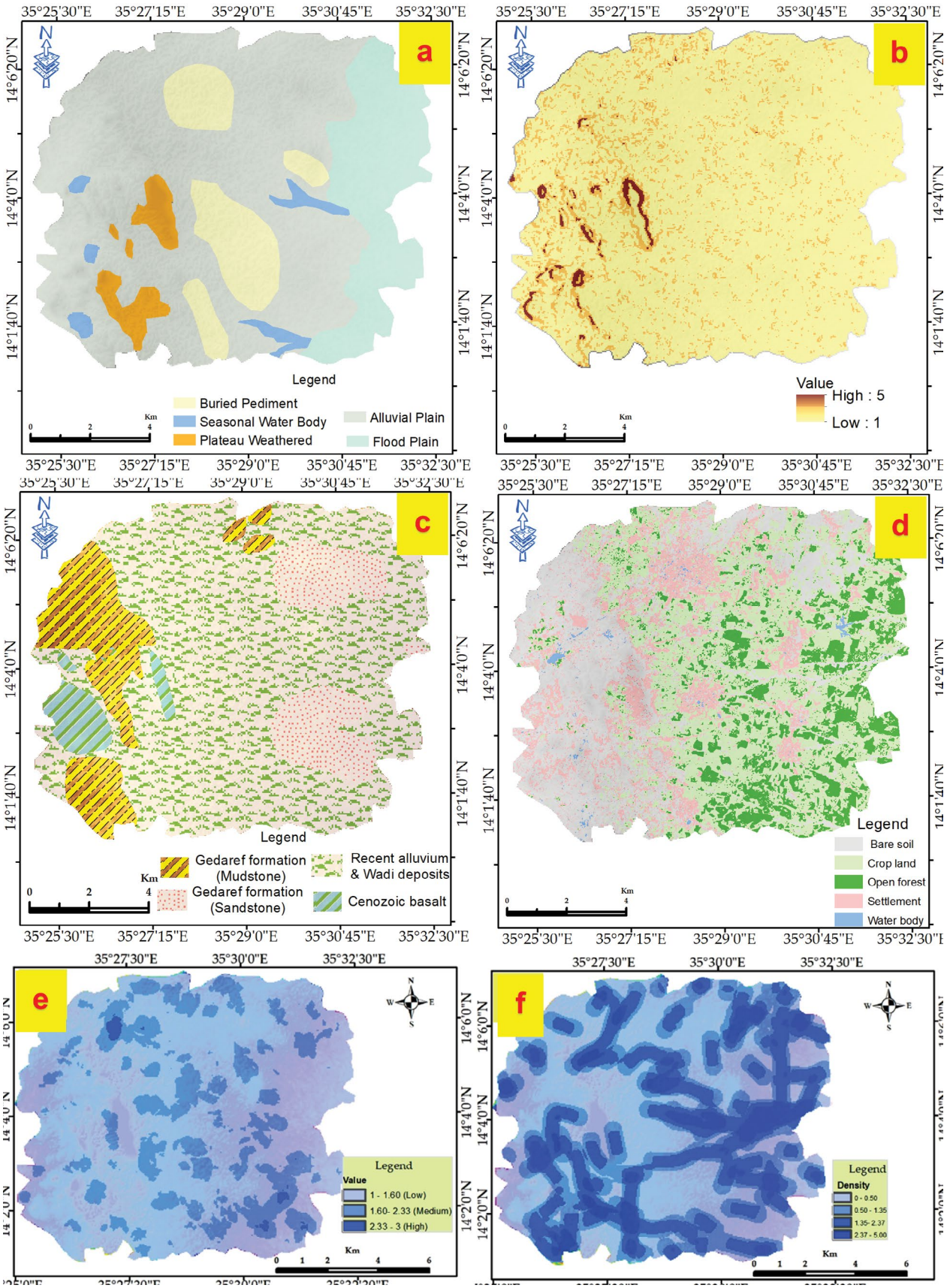

Fig. 3. (a) Geomorphology, (b) slope, (c) geology, (d) land use, (e) drainage density, and (f) lineaments density.

Table 1
Weights and rankings of different thematic layers

Thematic layer	Weight	Normalized weight	Class	Rank	Normalized rank
Geomorphology	7	0.226	Plateau weathered	7	0.189
			Flood plain	9	0.243
			Seasonal water body	10	0.270
			Alluvial plain	6	0.162
			Buried pediment	5	0.135
Slope (%)	2	0.065	<1	9	0.450
			1–3	7	0.350
			>3	4	0.200
Geology	8	0.258	Recent alluvium & wadi deposits	5	0.217
			Cenozoic basalt	3	0.130
			Gedaref formation (mudstone)	6	0.261
			Gedaref formation (sandstone)	9	0.391
Land use/land cover	5	0.161	Cropland	6	0.231
			Settlements	2	0.077
			Open forest	6	0.231
			Bare soil	2	0.077
			Water bodies	10	0.385
Lineament density (m/km$_2$)	6	0.194	2.37–5.00	10	0.357
			1.35–2.37	8	0.286
			0.50–1.35	7	0.250
			0–0.50	3	0.107
Drainage density (m/km$_2$)	3	0.097	2.33–3	8	0.296
			1.60–2.33	9	0.333
			1–1.60	10	0.370

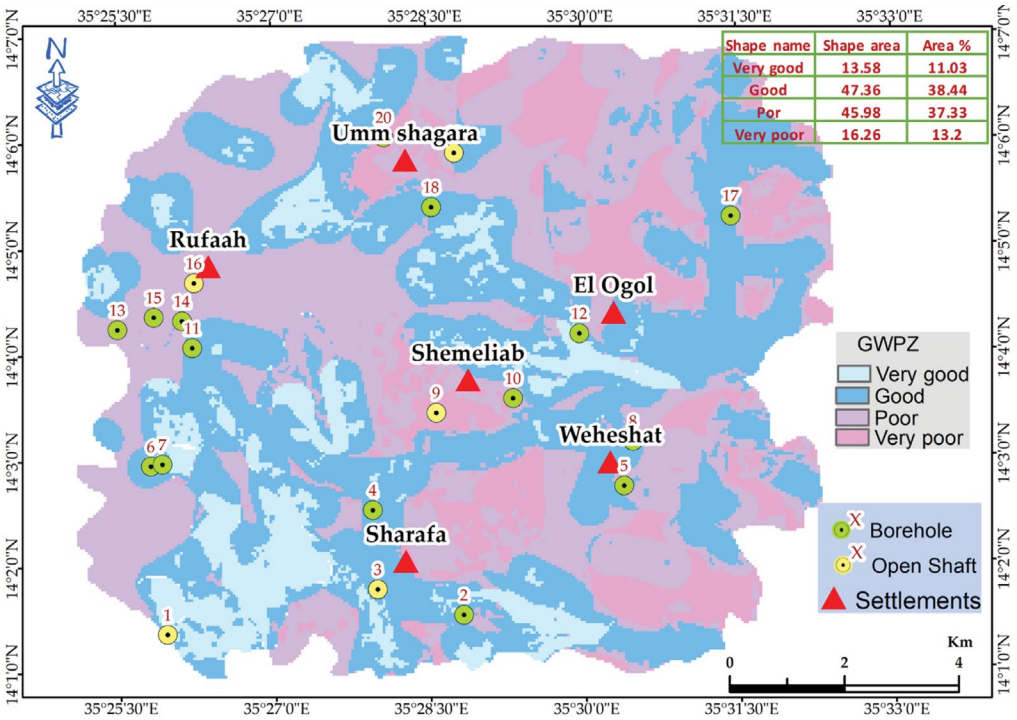

Fig. 4. Groundwater potential zone map of the study area.

Table 2
Results of the interpreted VES curves

		VES01	VES02	VES03	VES04	VES05	VES06	VES07	VES08	VES09	VES10	VES11
Resistivity (p–m)	P1	8.1	6.11	7.23	7.23	7.9	7.19	10.7	11.5	5.17	3.95	6.98
	P2	50	15.7	111.4	209	1,231	4.33	6.24	579	11.5	62.9	103
	P3	142	107	168.6	62.9	44.9	147	96.8	91.7	376.3	238	230
	P4	66.8	85	38.39		83.1	60.3	122	164	115.5	47.5	16.9
	P5	–	–	–	–	–	16,600	–	53.8	77.76	–	–
Thickness (h–m)	h1	3.19	2.38	4.54	5.54	6.37	0.737	0.747	3.99	0.76	2.14	4.88
	h2	8.36	3.5	30.2	171	18.4	2.86	2.61	8.76	3.81	45.2	91.6
	h3	256	245	237.7		138	131	67.9	83.1	11.54	83.2	255
	h4	–	–	–	–	–	279	–	141	164.7	–	–
Depths (d–m)	d1	3.19	2.38	4.54	5.54	6.37	0.737	0.747	3.99	0.76	2.14	4.88
	d2	11.5	6.48	334.73	177	24.8	3.6	3.35	12.8	4.58	47.3	96.5
	d3	267	251	272.4		163	135	71.3	95.9	16.11	130	352
	d4	–	–	–	–	–	279	–	237	180.8	–	–
Curve type		AK	AK	AK	K	KQ	HKH	HA	KHK	AKQ	AK	AK

3.2.1. Electrical resistivity survey

The resistivity survey of the investigation conducted through two denomination field methods. These methods are VES for vertical variations and HEP, for lateral variations. VES sounding operates a collinear array which produced a 1-D vertical apparent resistivity against the depth at a particular measurement point. Eleven VES was conducted in the Shemeliab watershed area to investigate the groundwater aquifer's characteristics and to realize the variation of subsurface lithology. Schlumberger arrangement was performed to obtain information about the vertical lithological variations and aquifer depths.

3.2.1.1. Vertical electrical sounding VES curves interpretation

Seven curve types were detected from eleven VES (Table 2); namely: *K*-type curve ($\rho1 < \rho2 > \rho3$) for one station; VES-4, AK type curves ($\rho1 < \rho2 < \rho3 > \rho4$) for five stations; VES-1, VES-2, VES-3, VES-10, and VES-11, HA type curve ($\rho1 > \rho2 < \rho3 < \rho4$) for one station; VES-7, KQ type curve ($\rho1 < \rho2 > \rho3 > \rho4$) one station; VES-5, AKQ type curve ($\rho1 < \rho2 < \rho3 > \rho4 > \rho5$) one station; VES-9, HKH type curve ($\rho1 > \rho2 < \rho3 > \rho4 < \rho5$) one station; VES-6 and KHK type curve ($\rho1 < \rho2 > \rho3 < \rho4 < \rho5$) one station VES-6.

The resistivity measuring results reveal that there are many layers type of the Shemeliab area showed in Fig. 5a. The geoelectrical layers of *K*-type curve could interpret as three subsurface layers: superficial deposits, basalt, and sandstone. The resistivity ρ-values vary from 7.23 to 209 Ohm m. The thickness *h* varies from 5.54 to 171 m while the depth *d* reaches up to 177 m. The interpreted of four subsurface layers in AK, HA, and KQ, interpreted as superficial deposits, weathered basalt, fresh basalt, and sandstone. The five layers of HKH and KHK curves were observed in (VES6) and (VES8). The resistivity values of the HKH type curve has a range between 4.33–16,600 Ohm m, the top bedrock has 279 m thickness. The layer successions were interpreted as (Superficial deposits, weathered basalt, fresh basalt, sandstone, and basement rock). The KHK curve included seven different layers that were interpreted as, (Superficial deposits, weathered basalt, fresh basalt, sandstone, and saturated clay).

3.2.1.2. Electrical resistivity tomography

The purpose of using resistivity tomography procedure was to form the geometry of the subsurface geology (lithology units and groundwater zones). The Wenner–Schlumberger array electrode arrangement utilized for horizontal variation and vertical investigations. The profiles handled in the Shemeliab area was oriented to cross the target fractures (release and extensional fractures). The descriptions of each resistivity profiles, their resistivity relationships, and analysis specified in the following:

3.2.1.3. Profile one

This profile extended along VES-05 and VES-8 trending NE-SW, with a total extent of 960 m with 10 m electrode spacing (Fig. 5b). Apparent resistivity inverted to a penetrating depth of 115 m. The topsoil of superficial deposits and thick clay with a thickness of approximately 19 m, shows large variations of the resistivity values suggest that the soil materials are inhomogeneous. Below 19 m, the saturated zone of the clay layer starts with slightly brackish water till 86 m depth. The basaltic rocks are capping the sandstone aquifer which begins from a depth below 90 m characterized by low resistivity value indicating a presence of salinity zone.

3.2.1.4. Profile two

Fig. 5c shows an example of the obtained models at sounding No. 3 correlated with the nearby borehole Shemeliab borehole (Sh-BH1). Correlation of the derived models with geologic borehole information indicates that there is an exists of four layers; fresh basal, weathered basalt, and superficial soil. This profile passed through

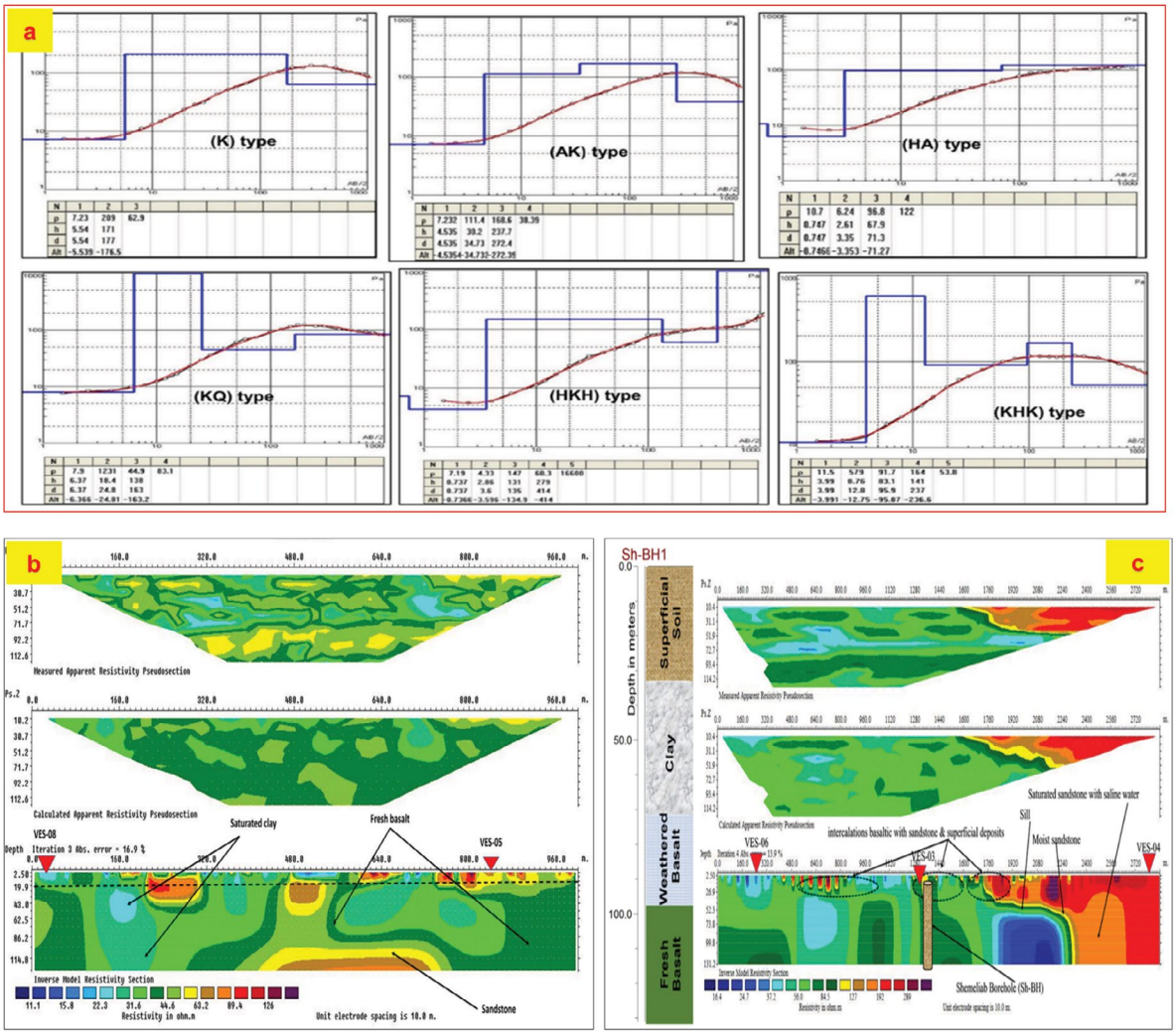

Fig. 5. (a) VES type curves, (b and c) electrical tomography images – profile 1 and 2 of the Shemeliab watershed area.

three VES points, VES-04, VES-03, and VES-6 with a proximate length of 3 km with 10 m electrode spacing. Apparent resistivity reached a depth of 131 m. The topsoil reflects a very high variation of resistivity values due to intercalations of Oligocene basaltic with sandstone and superficial deposits with a thickness of approximately 21 m. However, in some parts the basalt is formed as a sill layer capped the sandstone. Below 21 m, the saturated zone of the clay layer starts with slightly brackish water. The eastern part of this profile represents a thick layer of sandstone with a resistivity higher than 300 Ohm m interpreted as moist sandstone, decreasing downward with resistivity value 192 Ohm m, which was defined as saturated sandstone with slightly saline water.

3.2.2. *Validation using wells inventory and electrical resistivity data*

The developed model validation was checked against both: (1) the interpreted geophysical data, and (2) the boreholes data. Thus, in this case the wells yield data, and the resistivity data have been overlaid with the final map to authenticate the model. The interpolation of the geophysical interpretation was reproduced as a polygon feature class using ArcGIS.V10.5. However, we used the ArcToolbox to produce rectangular cells of a regularly spaced grid of sampling points inside a polygon layer with 1 km desired points spacing shown in Fig. 6a. A total of 156 points has been classified according to the interpretation of subsurface lithology and their compatibility to the groundwater occurrence, for example, the sandstone has very good compatibility, the saturated clay was relatively classified as good, weathered basalt signed as poor and the fresh basalt was classified as very poor. The classified points of the reported locations were overlaid and correlated with the GWPZ model depicted in Fig. 6b. The model generated an output map of the groundwater potential zone is further validated with the data related to yield potentialities of different borehole/open shaft wells in the study area (Table 3). The correlated data from borehole/open shaft wells proved a good correlation with the ultimate output model.

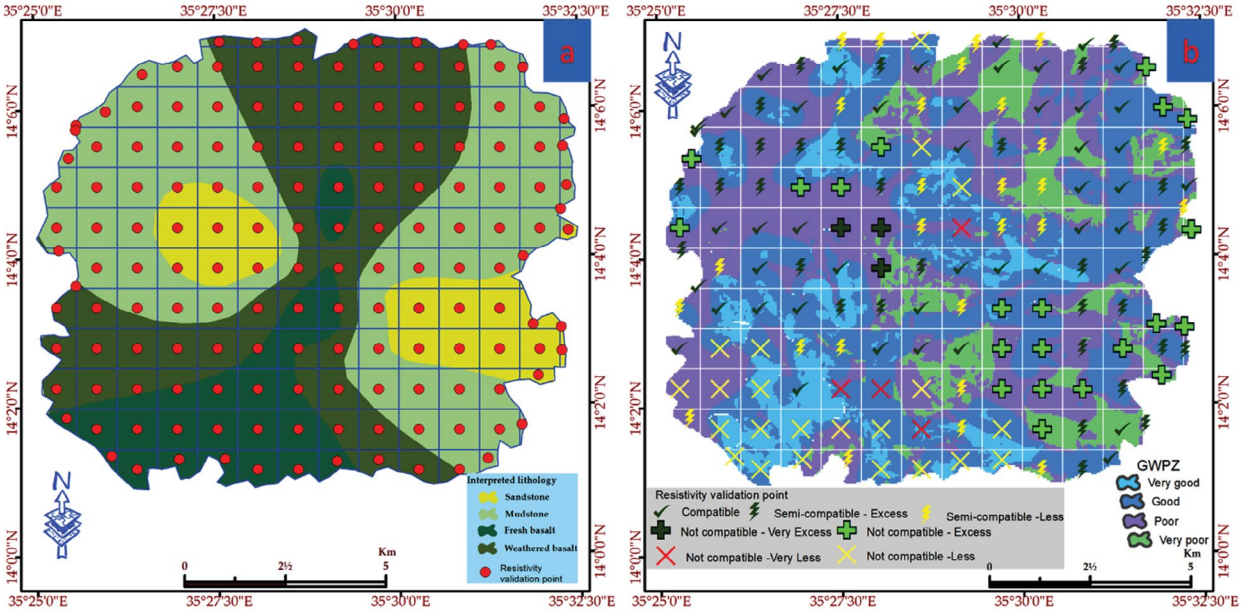

Fig. 6. (a) Produced resistivity validation sampling points and (b) resistivity validation point correlated with the GWPZ model.

Table 3
Yields of different borehole/open shaft well correlated with GWPZ model in the study area

ID	Name	Type	Longitude	Latitude	Yield G/h	Class yield	Model yield	Remarks
1	Dalasa Ghanga	Open shaft	762726.514	1551586.887	3,100	Very good	Very good	Compatible
2	Umm Shega	Borehole	767889.105	1551933.906	2,100	Good	Good	Compatible
3	Sharafa	Open Shaft	766387.511	1552379.116	3,300	Very good	Good	Semi-compatible – excess
4	Wad Eddam	Borehole	766303.311	1553760.005	2,200	Good	Good	Compatible
5	Elsherafa	Borehole	770681.404	1554189.757	850	Poor	Poor	Compatible
6	Wad Eddam	Borehole	762431.562	1554517.287	1,000	Poor	Good	Semi-compatible – less
7	Wad Eddam	Borehole	762634.760	1554548.900	3,300	Very good	Very good	Compatible
8	Wad Elsyi	Borehole	770834.560	1554965.022	720	Poor	Good	Semi-compatible – less
9	Elshemalyab	Open shaft	767409.054	1555452.806	963	Very poor	Very poor	Compatible
10	Esh-shamal	Borehole	768742.772	1555708.542	720	Poor	Poor	Compatible
11	Elseraf-1	Borehole	763153.747	1556578.532	2,100	Good	Good	Compatible
12	Wad Eddam	Borehole	769900.516	1556837.165	2,100	Good	Good	Compatible
13	Elseraf	Borehole	761846.983	1556893.065	3,100	Very good	Poor	Not compatible – excess
14	Esh-shemal	Borehole	762976.374	1557046.777	2,300	Good	Poor	Semi-compatible – excess
15	Rufaa	Borehole	762480.489	1557108.072	917	Por	Poor	Compatible
16	Rufaa	Open shaftl	763183.847	1557707.564	2,300	Good	Poor	Semi-compatible – excess
17	Elangul-1	Borehole	772537.817	1558892.878	2,210	Good	Good	Compatible
18	Umm Shaga	Borehole	767313.762	1559034.779	1,916	Good	Good	Compatible
19	Umm Shagara	Open shaft	767710.221	1559984.701	3,500	Very good	Good	Semi-compatible – excess
20	Umm Shagr	Borehole	766483.396	1560252.970	420	Very poor	Very poor	Compatible

4. Conclusion

In this study, the RS data has been used successfully coupled with a GIS scheme to gain a detailed understanding of the groundwater situation in the Shemeliab watershed area. The output thematic map was categorized in four GWPZ – very good, good, poor, and very poor, the matching areal coverage and percentage in each group were about 13.58 (11.03%), 47.36 (38.44%), 45.98 (37.33%), and 16.26 (13.20%) km^2 out of the total areal extent of 123.19 km^2. The developed model validation was checked against the interpreted geophysical data and the boreholes data which gives the current groundwater yields. Thus, the correlations confirmed that there is good compatibility of the present study

in determining the GWPZ in the Shemeliab watershed area. The techniques used in this study explain the applicability and eligibility in defining the GWPZ of the various geological units in the Shemeliab watershed area. The study has added considerably useful information at a detailed scale that generally not practiced during geological investigations; for example, it can add up to the existing geological information in the study area. However, the presented study is not only applicable to the Shemeliab area but also it could be used in other regions that have the same environmental and geological situations.

Funding

This work was supported by the Sichuan Environmental Engineering Assessment Centre Project Technical Consultation on Comprehensive Assessment of Groundwater Pollution Status in Typical Industrial Park of Shiyang, Deyang (2017H01013).

Acknowledgments

The authors thank the Water Corporation of Gedaref State – Sudan (WCGSS) and Water Environmental Sanitation (WES), Project Gedaref State – Sudan for the technical support of this study.

References

[1] B.A. Elubid, T. Huang, E.H. Ahmed, J. Zhao, M. Elhag, W. Abbass, M.M. Babiker, Geospatial distributions of groundwater quality in Gedaref state using geographic information system (GIS) and drinking water quality index (DWQI), Int. J. Environ. Res. Public Health, 16 (2019) 731.
[2] A. Stampolidis, P. Tsourlos, P. Soupios, T. Mimides, G. Tsokas, G. Vargemezis, A. Vafidis, Integrated geophysical investigation around the brackish spring of Rina, Kalimnos Isl., SW Greece, J. Balkan Geophys. Soc., 8 (2005) 63–73.
[3] D. Jhariya, Groundwater prospect mapping using remote sensing, GIS and resistivity survey techniques in Chhokra Nala Raipur district, Chhattisgarh, India, J. Water Supply Res. Technol. AQUA, 68 (2019) 595–606.
[4] N. Allouche, F. Ben Brahim, M. Gontara, H. Khanfir, S. Bouri, and Technology-Aqua, Validation of two applied methods of groundwater vulnerability mapping: application to the coastal aquifer system of Southern Sfax (Tunisia), J. Water Supply Res. Technol. AQUA, 64 (2015) 719–737.
[5] S. Saidi, S. Bouri, S. Hassine, H. Ben Dhia, Comparison of three applied methods of groundwater vulnerability mapping: application to the coastal aquifer of Chebba–Mellouleche (Tunisia), Desal. Water Treat., 52 (2014) 2120–2130.
[6] S.I. Elmahdy, M.M. Mohamed, Groundwater potential modeling using remote sensing and GIS: a case study of the Al Dhaid area, United Arab Emirates, Geocarto Int., 29 (2014) 433–450.
[7] R.M. Teeuw, Groundwater exploration using remote sensing and a low-cost geographical information system, Hydrogeol. J., 3 (1995) 21–30.
[8] S. Shekhar, A.C. Pandey, Delineation of groundwater potential zone in hard rock terrain of India using remote sensing, geographical information system (GIS) and analytic hierarchy process (AHP) techniques, Geocarto Int., 30 (2015) 402–421.
[9] S. Lee, Y. Hyun, M.-J. Lee, Groundwater potential mapping using data mining models of big data analysis in Goyang-si, South Korea, Sustainability, 11 (2019) 1678.
[10] P.K. Srivastava, A.K. Bhattacharya, Groundwater assessment through an integrated approach using remote sensing, GIS and resistivity techniques: a case study from a hard rock terrain, Int. J. Remote Sens., 27 (2006) 4599–4620.
[11] M. Oladunjoye, A. Adefehinti, K. Ganiyu, Geophysical appraisal of groundwater potential in the crystalline rock of Kishi area, Southwestern Nigeria, J. Afr. Earth Sci., 151 (2019) 107–120.
[12] H.S. Virupaksha, K.N. Lokesh, Electrical resistivity, remote sensing and geographic information system approach for mapping groundwater potential zones in coastal aquifers of Gurpur watershed, Geocarto Int., (2019) 1–15.
[13] I. Nouioua, A. Rouabhia, C. Fehdi, M. Boukelloul, L. Gadri, D. Chabou, R. Mouici, The application of GPR and electrical resistivity tomography as useful tools in detection of sinkholes in the Cheria Basin (Northeast of Algeria), Environ. Earth Sci., 68 (2013) 1661–1672.
[14] M. Van Schoor, Detection of sinkholes using 2D electrical resistivity imaging, J. Appl. Geophys., 50 (2002) 393–399.
[15] E.-S. El-Bushra, The Urban Crisis and Rural-Urban Migration in Sudan, B. Potter Robert, Unwin Tim, Eds., The Geography of Urban-Rural Interaction in Developing Countries, Routledge, London, New York, NY, 2017, pp. 109–140.
[16] S.B.M. Ahmed, A.F. Ahmed, Genotype season interaction and characters association of some Sesame (*sesamum indicum* L.) genotypes under rain-fed conditions of Sudan, Afr. J. Plant Sci., 6 (2012) 39–42.
[17] D. Almond, O. Kheir, S. Poole, Alkaline basalt volcanism in Northeastern Sudan: a comparison of the Bayuda and Gedaref areas, J. Afr. Earth Sci., 2 (1984) 233–245.
[18] D. Almond, The relation of Mesozoic-Cainozoic volcanism to tectonics in the Afro-Arabian dome, J. Volcanol. Geotherm. Res., 28 (1986) 225–246.
[19] K. Ibrahim, M. Hussein, I. Giddo, Application of combined geophysical and hydrogeological techniques to groundwater exploration: a case study of Showak-Wad Elhelew area, Eastern Sudan, J. Afr. Earth Sci., 15 (1992) 1–10.
[20] M. Hussein, E. Adam, Water quality of the Gedaref basin, Sudan, Hydrol. Sci. J., 40 (1995) 205–216.
[21] M. Mirghani, Concepts and Models for the Characterization of the West Gedaref Hydrogeologic System, Sudan, Vol. 22, Ph.D. Thesis, Technische Universität Berlin, Ehemalige Fakultät VI–Bauingenieurwesen und Angewandte Geowissenschaften, Technische Universität Berlin, Berlin, 2002, pp. 133.
[22] A. Eisawi, E. Schrank, Terrestrial palynology and age assessment of the Gedaref formation (Eastern Sudan), J. Afr. Earth Sci., 54 (2009) 22–30.
[23] A.A. Eisawi, I.A. Babikir, K.A.O. Salih, Paleoecological significance of newly discovered trace fossils near the Gedaref town, Eastern Sudan, J. Afr. Earth Sci., 61 (2011) 233–237.
[24] A.F.I. Osman, A. Ibrahim, Y. Abuobida, A.A.M. Eisawi, M. Alhadi, O. Mukhtar, A.A. El Tijani, Sedimentary facies and depositional environment of the Gedaref formation, Eastern Sudan, Am. J. Earth Sci., 2 (2015) 236–241.
[25] A. Kröner, Ophiolites and the evolution of tectonic boundaries in the late proterozoic Arabian—Nubian shield of Northeast Africa and Arabia, Precambrian Res., 27 (1985) 277–300.
[26] T. Saaty, Decision making with the analytic hierarchy process, Int. J. Serv. Sci., 1 (2008) 83–98.